Self-junctioned copper nanofiber transparent flexible conducting film via electrospinning and electroplating

Seongpil An[+], Hong Seok Jo[+], Do-Yeon Kim, Hyun Jun Lee, Byeong-Kwon Ju, Salem S. Al-Deyab, Jong-Hyun Ahn, Yueling Qin, Mark T. Swihart, Alexander L. Yarin, Sam S. Yoon**

S An,[+] HS Jo, [+] DY Kim, Prof. AY Yarin, Prof. SS Yoon
School of Mechanical Engineering
Korea University
Seoul 02841, Republic of Korea
E-mail: skyoon@korea.ac.kr; ayarin@uic.edu
Dr. HJ Lee, Prof. BK Ju
Display and Nanosystem Laboratory
Korea University
Seoul 02841, Republic of Korea
Prof. SS Al-Deyab
Petrochemicals Research Chair, Department of Chemistry, College of Science
King Saud University
Riyadh 11451, Saudi Arabia
Prof. JH Ahn
School of Electrical and Electronic Engineering
Yonsei University
Seoul 03722, Republic of Korea
Dr. Yueling Qin
Department of Physics
University at Buffalo, The State University of New York
Buffalo, New York 14260-4200, USA.
Prof. MT Swihart
Department of Chemical and Biological Engineering
University at Buffalo, The State University of New York
Buffalo, New York 14260-4200, USA
Prof. AY Yarin
Department of Mechanical and Industrial Engineering
University of Illinois at Chicago
Chicago, Illinois 60607-7022, USA
[+]These authors equally contributed to the work

Keywords: electrospinning, electroplating, transparent conducting electrode, percolation model

Numerous existing and emerging devices, including light-emitting diodes (LEDs),[1] organic LEDs,[2] displays,[3] touch screens,[4] solar cells,[5] smart windows,[6] and interactive electronics[7, 8] require transparent conducting electrodes (TCEs) that combine high transparency (T) with low sheet resistance (R_s). These requirements are mutually incompatible, as low R_s relies on high mobility charge carriers that inevitably interact with light and reduce T. Indium-doped tin oxide (ITO), a mechanically stable and reliable material that provides a reasonable tradeoff between R_s and T, dominates commercial TCE applications. However, the rising cost and diminishing supply of indium, along with the rigidity and brittleness of ITO, limit use in low-cost flexible devices such as wearable electronics, flexible solar cells, roll-up displays, and electronic skins.[9]

Nanostructured materials including carbon nanotubes (CNTs),[3, 10, 11] graphene,[4, 12-14] metal nanofibers,[9, 15-17] and conductive polymers[18] have been proposed as ITO replacements. For CNT films, R_s is typically an order of magnitude higher than that of ITO.[19, 20] Chemical vapor deposition (CVD) grown graphene can outperform ITO,[4] but requires a multi-step growth-and-transfer fabrication process that limits its applicability. Metal nanowires (NWs) show great promise, achieving high transparency using nanostructures smaller than the wavelengths of visible light, while metallic conductivity allows low R_s with sparse NW coverage. Metal NW films have achieved $R_s = 10\ \Omega$/sq at $T \geq 90\%$.[21, 22] However, further improvement has been limited by high contact resistance at NW intersections. This junction resistance is the central challenge for all one-dimensional percolative materials, including those based on CNTs. Eliminating it requires producing a continuous mesh without contact resistance at wire intersections. Previous studies have applied thermal post-processing or mechanical pressing to merge these junctions.[23, 24] However, these methods can damage the NWs and are incompatible with many low-cost, flexible substrates.

Wu *et al*. introduced copper nanofibers whose junctions were interconnected by thermally evaporated copper,[17] and were the first to achieve R_s < 10 Ω/sq with T > 90% using metal nanowires. Hsu *et al*. achieved R_s = 0.36 Ω/sq at T = 92% by combining mesoscale nanofibers with nanoscale metal wires.[16] However, the thermal evaporation used to link the nanowires with nanofibers is a high-vacuum process that may not be practical for low-cost production. Moreover, thermal post-treatment precludes the use of the flexible low-cost polymer substrates for flexible, stretchable, and rollable optoelectronic devices. Here we break through these limitations with an ultra-fast process for fabricating TCEs with a world record combination of low R_s and high T. This is achieved through electrospinning and electroplating for only a few seconds each, combining two high-throughput commercially-viable processes. When transferred to an Eco-flex substrate, these TCEs can be stretched by 580% with less than a factor of 5 increase in R_s, and can withstand more than 1000 cycles of bending to a 5 mm radius without appreciable increase in R_s. The performance demonstrated here exceeds that of Hsu *et al.*, while also eliminating the use of silver and maintaining compatibility with virtually any substrate, including thermally-sensitive polymers. The new approach demonstrated here could readily be incorporated into a continuous, roll-to-roll manufacturing sequence for low-cost, large-scale fabrication, because it can be implemented using only low-temperature, non-vacuum processing. Furthermore, we introduce a new model based on the renormalization technique of the percolation, which relates the electric conductivity and optical transmittance for the nanowire network.

Production of copper electroplated wire for transparent conducting electrodes (CuEW-TCEs) is illustrated in **Figure 1**. In electrospinning (**Figure 1**a**, 1**c) most of the solvent (dimethylformamide, DMF) is evaporated in flight and the solidified polymer (polyacrylonitrile, PAN) forms a self-intersecting mat from a single continuous nanofiber.[25] In the process of electroplating (**Figure 1**d), fiber junctions are bonded via metal deposition

on the outer surface of the platinum-seeded (**Figure 1**b) nanofibers. The electroplated copper fills the space around the crossed nanofibers (**Figure 2**a) which dramatically reduces contact resistance at the junctions. **Figure S2** shows cross-sections of the electroplated copper within a junction, demonstrating that the intersection is completely filled with dense electrodeposited copper, except for small pores corresponding to the original nanofibers. Drying in an inert atmosphere after electroplating is essential to the performance of the CuEW-TCEs. As shown in **Figure S3**, air drying produced substantial oxidation of the NWs and corresponding substantially reduced conductivity. However, once the NWs have been dried in an inert atmosphere, they are stable in air and their performance does not degrade upon air exposure. For these reasons, excellent electrical performance of CuEW-TCEs can be maintained even at locations such as a human skin or a leaf (**Figure 2**b, **Movie S1**). We measured single CuEW resistivity by transferring a CuEW to a bare substrate and contacting its ends with silver paint (**Figure S4**). Measurement on a single wire of ~1.8 μm diameter and ~250 μm length gave a resistivity of 6.7×10^{-8} Ω·m. This is within a factor of four of the resistivity of bulk copper, and is quite reasonable given the small diameter, rough surface, nanoscale grain size, possible surface oxidation, and presence of pores due to the electrospun fiber template within the CuEWs. This measurement provides a lower limit of the conductivity, because it is a two-point measurement that does not account for contact resistance between the wire and the silver paint electrodes or leads.

Figure 3 shows T versus R_s for the CuEW-TCEs on a polydimethylsiloxane (PDMS) substrate. T decreases from 97% to 41% as the first electrospinning time (t_{1st}) increases from 1 to 180 s (SEM images are shown in **Figure S5**), while R_s only decreases slightly, from 0.42 to 0.31 Ω/sq. Note that here the t_{1st} was varied at fixed electroplating time (3 s) and voltage (3 V). Thus, the total amount of copper deposited does not increase in proportion to t_{1st}. Even

though only a few CuEWs are deposited for t_{1st} = 1 s, R_s was already quite low, an outcome we attribute to the low junction resistance. In fact, R_s can be decreased to 0.138 Ω/sq when the electroplating time is increased to 7 s. However, T decreases as the electroplating time increases (**Figure S6**). Conversely, electroplating times below 3 s were insufficient to achieve complete electroplating. These results are superior to those reported in prior studies of Cu nanotroughs,[17] AuNFs,[9] graphene,[4] PEDOT:PSS,[22] SWNT,[26] and AgNW[27] as shown in **Figure 3**a. The removal of unplated support fibers (**Figure 1**f) is essential for achieving these high values of *T*. Although these nanofibers play an important role in protecting the metal-seeded nanofibers during electroplating, they scatter a significant amount of light; removing them significantly increases the transmittance (by 30%, **Figure S7**).

Figure 3e shows the transmittance spectra of all of the CuEW-TCEs (on PDMS substrates) after support fiber removal, showing uniform *T* over a wide range of wavelengths. This is enabled not only by the low coverage of CuEW, but also by the large size of the openings in the network (tens of μm, **Figure 2**a) relative to the wavelengths of visible light (hundreds of nm).[17] This flat transmittance spectrum is advantageous in many devices, including solar cells and photocatalytic water-splitting devices.

We conducted bending and stretching tests on the CuEW-TCEs, as shown in **Figure 4** and **Movies S2, S3, and S4**. The CuEW-TCEs on PET with t_{1st} = 5 and 30 s were used, and the sputtered ITO films on PET were prepared for comparison in bending tests. CuEW-TCEs maintained almost constant R_s as the bending radius (R_b) decreased from 100 to 1 mm. In contrast, for the ITO film, R_s increased dramatically at R_b = 10 mm and could not be measured for R_b < 6.5 mm (**Figure 4**a). Even after 1000 cycles of bending to R_b = 5 mm (**Figure 4**b) the CuEW-TCE retained its electrical conductivity, while R_s increased after a few cycles for the ITO film. **Figure 4**c, d show that CuEW-TCEs on Eco-flex also have

exceptional stretchability relative to previously reported TCEs.[9, 17] Lee et al.[28] achieved impressive results for a stretchable, though not very transparent, nanowire electrode, and showed that use of long nanowires was essential for improving stretchability. The electrospinning approach used here takes the concept of using long wires to the maximum possible extent by employing a continuous fiber; the remarkable stretchability results originate from the highly inter-connected structure of continuous electrospun nanofiber mats. The CuEW-TCEs samples were stretched up to 580% without a sharp rise in the value of $\Delta R/R_0$, which increases only to 3.6 for the sample with t_{1st} = 30 s. Even though some CuEWs are broken after stretching over 200%, the overall CuEW network maintains high conductivity through the many unbroken CuEWs even when stretched by 580% (**Figure S8**). As shown in **Movie S2**, electrical performance of CuEW-TCEs is retained under multi-directional stretching. The bulk resistance in the movie differs from the sheet resistance because the ohmmeter for bulk resistance reflects changes in the width and length of the sample as well as changes in sheet resistance.

A rigorous percolation model of the network of CuEWs on a surface is detailed in the Supporting Information. We can find the expected normalized conductivity C of the small six-point cell (**Figure S10**) or any larger cluster arising from it using the renormalization technique of the percolation theory (Eqs. S4 and S5) as

$$C = \frac{\bar{\sigma}}{\sigma_0} = \frac{1}{\sigma_0}\int_0^{\infty} \sigma P(\sigma) d\sigma = \frac{11}{3} p^3 (1-p)^2 + p^2 (1-p)^3 + \frac{17}{5} p^4 (1-p) + p^5 \qquad (1)$$

A large percolating cluster, which has $p \to 1$, according to Eq. 1 possesses conductivity $C \to p^5$, i.e. its conductivity tends to that of an individual copper nanowire. On the other hand, any large non-percolating cluster, which has inevitably $p \to 0$, possesses conductivity $C \to p^2$, which obviously tends to zero.

The predicted transmittance T is found accordingly as

$$T = 1 - \frac{\overline{B}}{S} = 1 - 5b\left[p(1-p)^4 + 4p^2(1-p)^3 + 6p^3(1-p)^2 + 4p^4(1-p) + p^5 \right] = 1 - 5bp \qquad (2)$$

Key parameters in this model are p, the probability that a link in the percolative network is occupied ($0 < p < 1$), and the shading factor b, the fraction of a cell ($0 < b < 1/5$) in the percolative network that is shaded by a single wire (a link in the network). If the dependence of the transmittance on resistance in the form of $Y = \log(T^{-0.5} - 1)$ versus $X = \log(1/C)$, as predicted by percolation theory, is superimposed at any constant shading factor b on the experimental results of the present work, the predictions of the percolations theory disagree with the data. The agreement is, however, possible when one finds an appropriate dependence of $b(p)$, with p being the probability of bond occupancy, as shown in **Figure 5**. The p values were obtained by substituting the dimensionless R ($=1/C$) by R_s/R_{single} in Eq. 1. The experimentally measured sheet resistance, R_s is in the 0.31 to 0.42 Ω/sq range and the numerically calculated resistance of a single CuEW is roughly $R_{single} = \rho L/A \sim 0.300$ Ω, where ρ, L, and A were 1.68×10^{-8} Ω·m (resistivity of copper), 12.8 μm (the average length between 200 intersections of CuEWs in SEM images), and 7.15×10^{-13} m^2 (the cross-sectional area of the copper-plated shell of a wire, when the total diameter of CuEW is 1000 nm and the core polymer diameter of CuEW is 300 nm), respectively. Then, b values were finally obtained by using Eq. 2, with the p values found using Eq. 1, and the experimental values of T. All of the values used and obtained are listed in **Table 1**. The p values range from 0.9759 to 0.8183 and the b values range from 0.1209 to 0.0073. The b values increase as t_{1st} increases, that is, the dimensionless factor b in the percolation model responsible for the shade of an individual nanofiber appears to be dependent on the deposition time in the experiment due to the nanofiber conglutination revealed by **Figure S8**. This provides a basis for understanding the

combined weak dependence of R_s and strong dependence of T upon the first electrospinning deposition time, which determines the total coverage of CuEWs in the TCE. Even at the shortest deposition time, p is already quite high, implying that a dense percolative network of highly conductive CuEWs has already formed. Thus further deposition dramatically increases b, the fraction of a cell shaded by a single link in the network, because the network becomes denser. However, it does not dramatically increase p, simply because p is already quite high.

In summary, we have presented a new approach to low-cost production of TCEs that can be used to generate films with unprecedented combinations of low R_s and high T while also providing exceptional mechanical flexibility and robustness. The key to the high performance of these CuEW-TCEs relative to other wire-based TCEs is the elimination of junction resistance at the intersection of wires, provided by the electroplating process used to deposit the copper wires. This disruptive advance in performance, robustness, and cost of TCEs opens up a vast array of new opportunities in flexible displays, electronic skins, and other low-cost, large area optoelectronic devices. Oxidation of CuEW-TCEs can be prevented by encapsulating the transparent conducting film between other device layers, as done in most optoelectronic devices.

Acknowledgements

This research was supported by Global Frontier Program through the Global Frontier Hybrid Interface Materials (GFHIM) of the National Research Foundation of Korea (NRF) funded by the Ministry of Science, ICT & Future Planning (2013M3A6B1078879), and the Industrial Strategic Technology Development Program (10045221) of MKE. This research was partially supported by the Commercializations Promotion Agency for R&D Outcomes (COMPA) funded by the Ministry of Science, ICT and Future Planning (MISP). S.S. Yoon expressed his thanks to the support made by King Saud University, Vice Deanship of Research Chairs. We appreciate the single wire conductivity measurement provided by Mr. Sujay Singh (UB).

Supporting Information

Supporting Information is available from Wiley Online Library or from the author.

References

[1] L. Li, Z. Yu, W. Hu, C. h. Chang, Q. Chen, Q. Pei, Adv. Mater. **2011**, 23, 5563.
[2] J. Wu, M. Agrawal, H. A. Becerril, Z. Bao, Z. Liu, Y. Chen, P. Peumans, ACS Nano **2009**, 4, 43.
[3] D. S. Hecht, L. Hu, G. Irvin, Adv. Mater. **2011**, 23, 1482.
[4] S. Bae, H. Kim, Y. Lee, X. Xu, J.-S. Park, Y. Zheng, J. Balakrishnan, T. Lei, H. R. Kim, Y. I. Song, Nature Nanotechnol. **2010**, 5, 574.
[5] Z. Yu, L. Li, Q. Zhang, W. Hu, Q. Pei, Adv. Mater. **2011**, 23, 4453.
[6] S. K. Deb, S.-H. Lee, C. E. Tracy, J. R. Pitts, B. A. Gregg, H. M. Branz, Electrochim. Acta **2001**, 46, 2125.
[7] D. J. Lipomi, M. Vosgueritchian, B. C. Tee, S. L. Hellstrom, J. A. Lee, C. H. Fox, Z. Bao, Nature Nanotechnol. **2011**, 6, 788.
[8] H. Peng, W. Dang, J. Cao, Y. Chen, D. Wu, W. Zheng, H. Li, Z.-X. Shen, Z. Liu, Nature Chem. **2012**, 4, 281.
[9] S. Soltanian, R. Rahmanian, B. Gholamkhass, N. M. Kiasari, F. Ko, P. Servati, Adv. Energy Mater. **2013**, 3, 1332.
[10] Z. Wu, Z. Chen, X. Du, J. M. Logan, J. Sippel, M. Nikolou, K. Kamaras, J. R. Reynolds, D. B. Tanner, A. F. Hebard, Science **2004**, 305, 1273.
[11] M. Zhang, S. Fang, A. A. Zakhidov, S. B. Lee, A. E. Aliev, C. D. Williams, K. R. Atkinson, R. H. Baughman, Science **2005**, 309, 1215.
[12] K. S. Kim, Y. Zhao, H. Jang, S. Y. Lee, J. M. Kim, K. S. Kim, J. H. Ahn, P. Kim, J. Y. Choi, B. H. Hong, Nature **2009**, 457, 706.
[13] G. Eda, G. Fanchini, M. Chhowalla, Nature Nanotechnol. **2008**, 3, 270.
[14] X. Li, G. Zhang, X. Bai, X. Sun, X. Wang, E. Wang, H. Dai, Nature Nanotechnol. **2008**, 3, 538.
[15] A. R. Rathmell, B. J. Wiley, Adv. Mater. **2011**, 23, 4798.
[16] P. C. Hsu, S. Wang, H. Wu, V. K. Narasimhan, D. Kong, H. R. Lee, Y. Cui, Nature Commun. **2013**, 4, 1.
[17] H. Wu, D. Kong, Z. Ruan, P.-C. Hsu, S. Wang, Z. Yu, T. J. Carney, L. Hu, S. Fan, Y. Cui, Nature Nanotechnol. **2013**, 8, 421.
[18] M. Vosgueritchian, D. J. Lipomi, Z. Bao, Adv. Funct. Mater. **2012**, 22, 421.
[19] J. Li, L. Hu, L. Wang, Y. Zhou, G. Grüner, T. J. Marks, Nano Lett. **2006**, 6, 2472.
[20] Y. Y. Huang, E. M. Terentjev, ACS Nano **2011**, 5, 2082.
[21] J. Lee, I. Lee, T. S. Kim, J. Y. Lee, Small **2013**, 9, 2887.
[22] T. Kim, Y. W. Kim, H. S. Lee, H. Kim, W. S. Yang, K. S. Suh, Adv. Funct. Mater. **2013**, 23, 1250.
[23] W. Gaynor, G. F. Burkhard, M. D. McGehee, P. Peumans, Adv. Mater. **2011**, 23, 2905.
[24] E. C. Garnett, W. Cai, J. J. Cha, F. Mahmood, S. T. Connor, M. G. Christoforo, Y. Cui, M. D. McGehee, M. L. Brongersma, Nature Mater. **2012**, 11, 241.
[25] A. L. Yarin, B. Pourdeyhimi, S. Ramakrishna, *Fundamentals and applications of micro and nanofibers*, Cambridge University Press, **2014**.
[26] V. Scardaci, R. Coull, J. N. Coleman, Appl. Phys. Lett. **2010**, 97, 023114.
[27] S. De, P. J. King, P. E. Lyons, U. Khan, J. N. Coleman, ACS Nano **2010**, 4, 7064.
[28] P. Lee, J. Lee, H. Lee, J. Yeo, S. Hong, K. H. Nam, D. Lee, S. S. Lee, S. H. Ko, Adv. Mater. **2012**, 24, 3326.

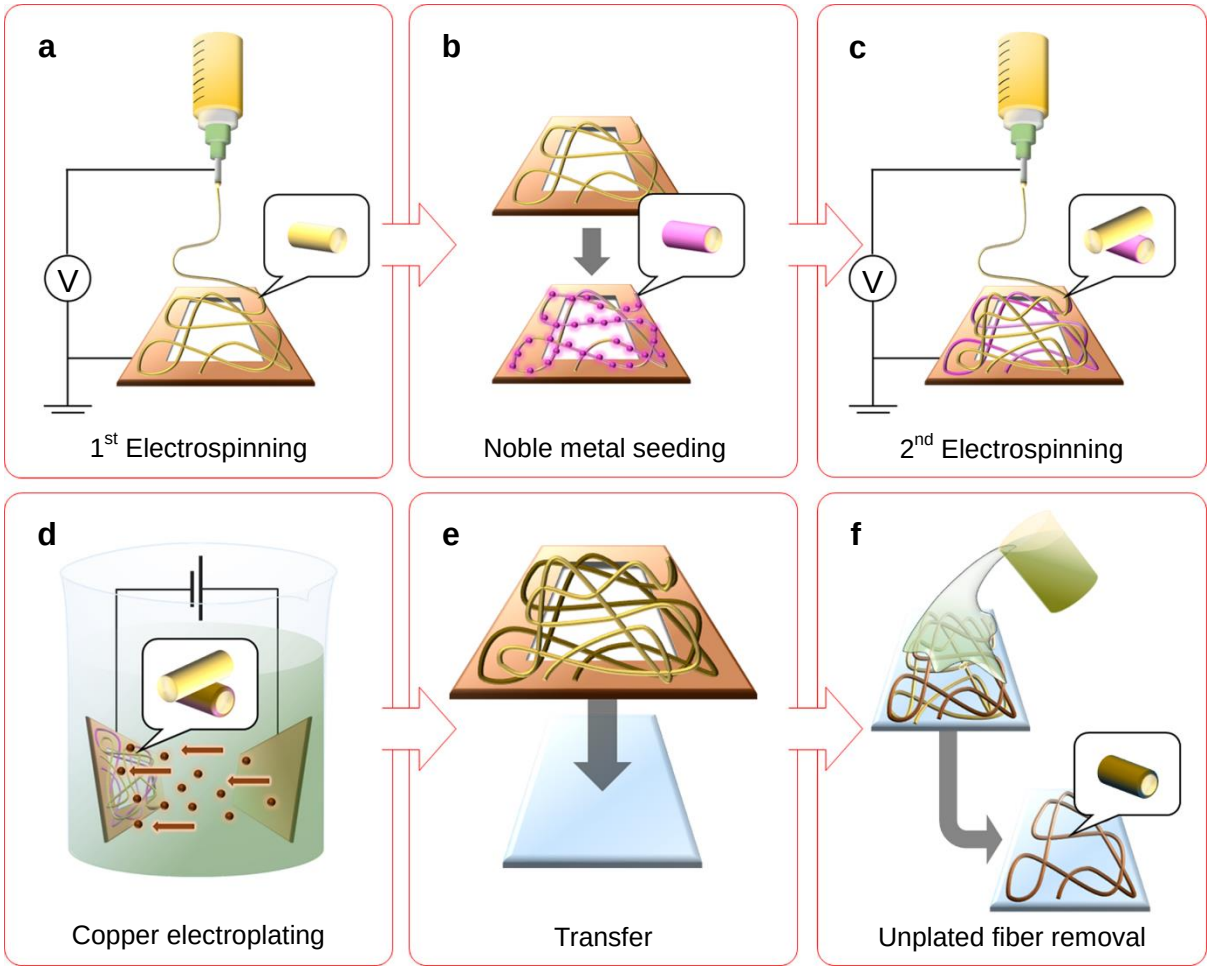

Figure 1. Schematic of the fabrication process for CuEW-TCEs. a) The first electrospun polymer nanofibers are deposited onto a copper frame. b) The nanofibers are made conductive by noble metal seeding. c) The second layer of electrospun polymer nanofibers is deposited above the platinum-seeded nanofibers. d) Only the metal-seeded nanofibers are electroplated by copper. (The second layer of electrospun nanofibers is not electroplated, because without platinum seeding they are non-conductive). e) The electroplated and non-electroplated nanofibers are transferred to a transparent substrate. f) The non-electroplated nanofibers are removed by dissolution.

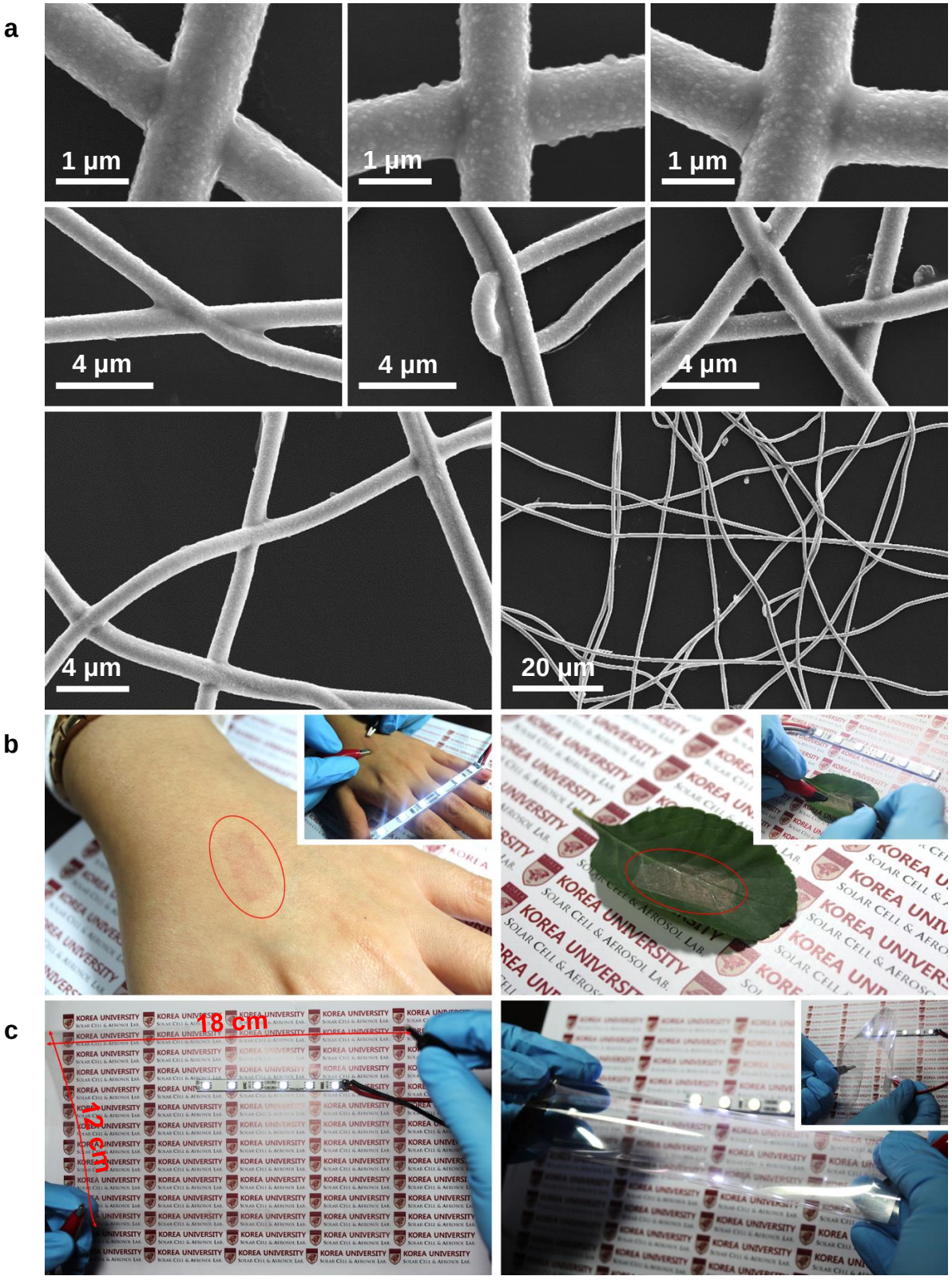

Figure 2. Copper electroplated wire (CuEW) for transparent conducting electrodes (TCEs). a) SEM images of CuEW-TCEs on PDMS. b) Images of CuEW-TCEs (duration of the first electrospinning stage t_{1st} = 30 s) transferred to a human hand and a leaf (a movie showing LED operation is provided in Supporting Movie as **Movie S1**). c) Images of large-scale CuEW-TCEs on PET (t_{1st} = 10 s).

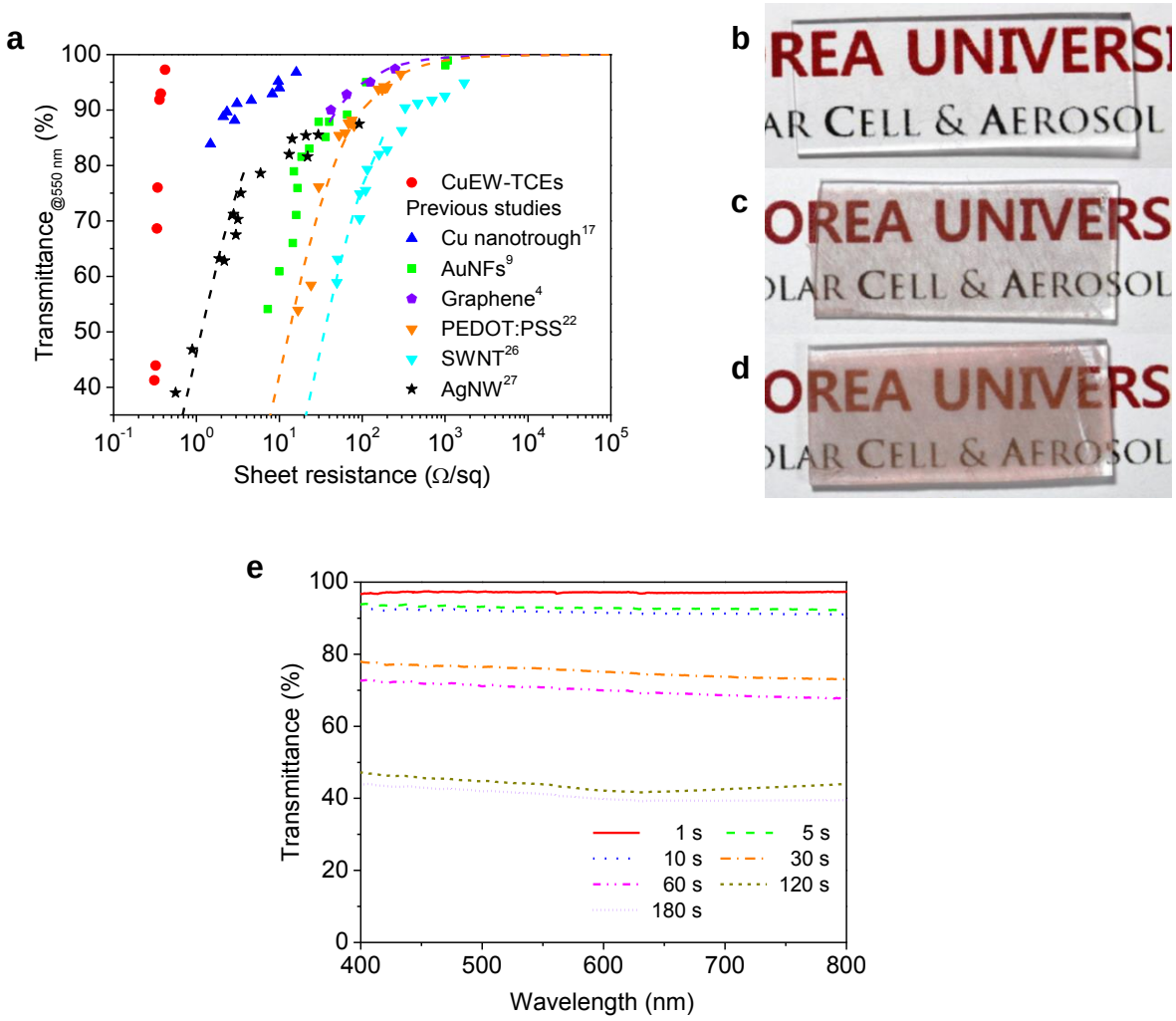

Figure 3. Optical and electrical performance. a) Transmittance versus sheet resistance for the CuEW-TCEs in comparison to prior studies. Images of CuEW-TCEs on PDMS with first electrospinning time: b) t_{1st} = 1 s, c) t_{1st} = 60 s, and d) t_{1st} = 180 s. e) Transmittance spectra of CuEW-TCEs after removal of unplated support fibers.

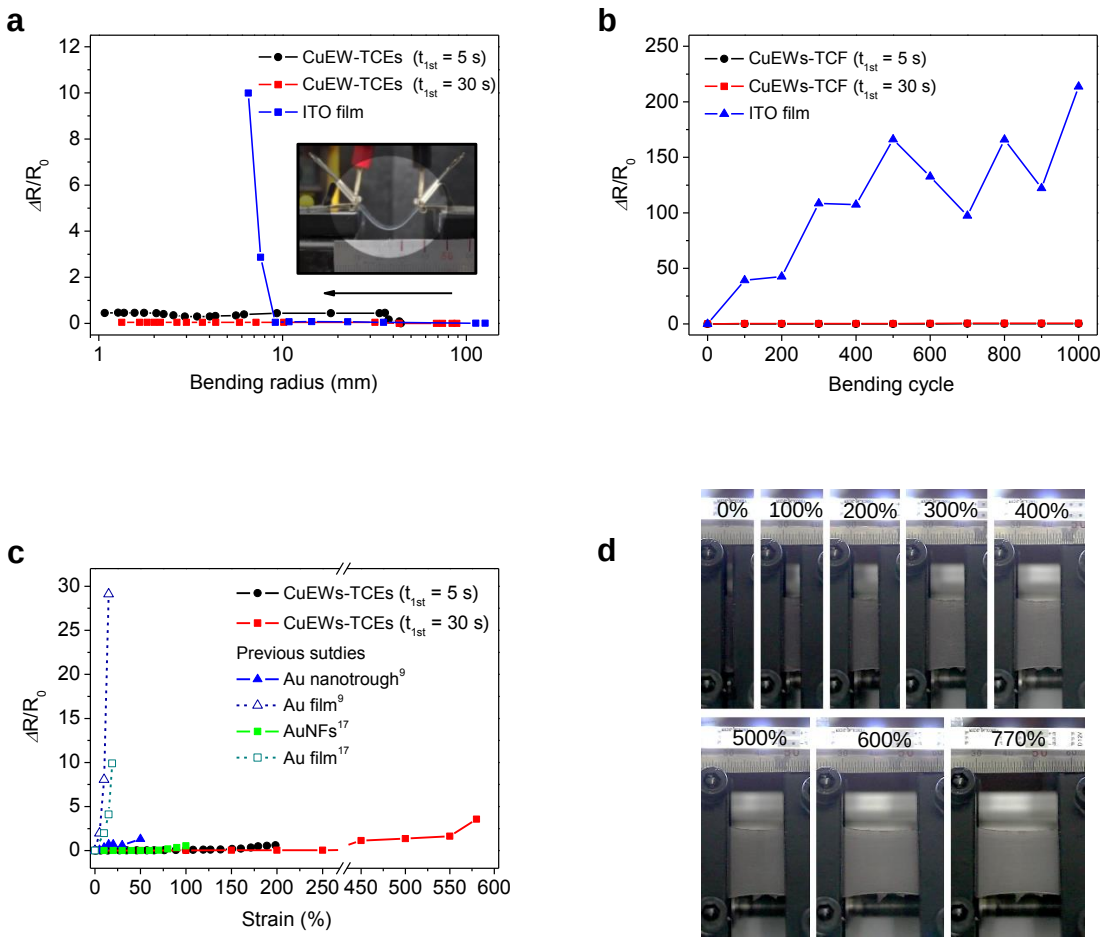

Figure 4. Mechanical stability. Changes in the sheet resistance as a function of: a) bending radius, b) bending cycle (CuEW-TCEs on PET), and c) unaxial strain in tensile test of CuEW-TCEs on Eco-flex d) Images of CuEW-TCEs on Eco-flex during stretching up to 770% (a movie showing LED operation is provided in Supplementary Materials as **Movie S3**).

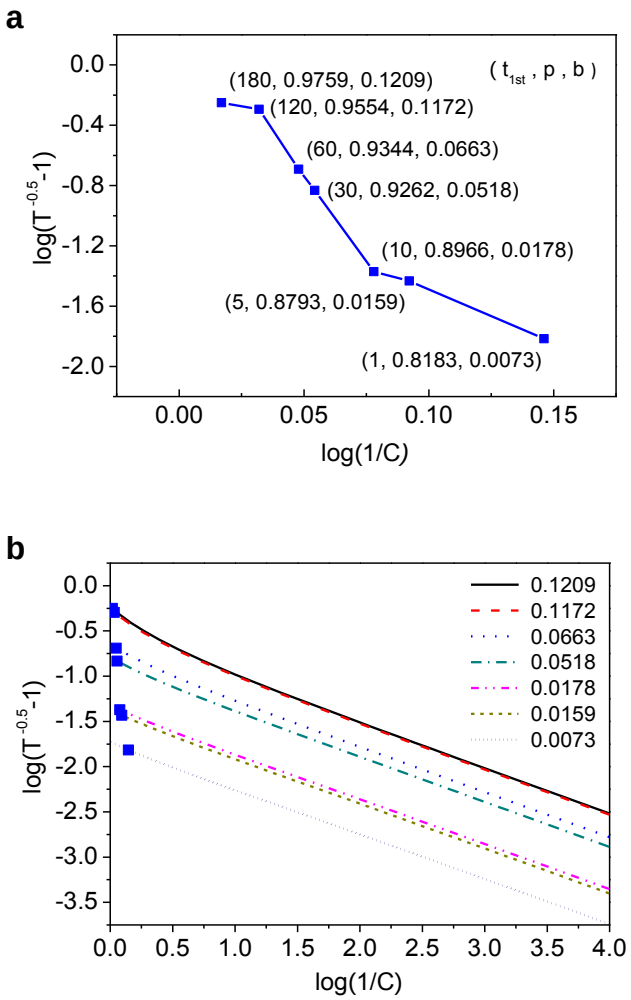

Figure 5. Percolation model of conductance and transmittance. Dependence of transmission on resistance: a) Experimental data and the corresponding values of *p* and *b* found from the percolation theory. b) Theoretical results based on Eqs. (3) and (7), with each line corresponding to a constant value of *b*; blue symbols correspond to the theoretical results from panel a).

Case	*Experimental result*		*Percolation model*			
t_{1st} (s)	R_s (Ω/sq)	T (%)	R	T	p	b
180	0.312	41	1.04	41	0.9759	0.1209
120	0.323	44	1.08	44	0.9554	0.1172
60	0.335	69	1.12	69	0.9344	0.0663
30	0.340	76	1.13	76	0.9262	0.0518
10	0.359	92	1.20	92	0.8966	0.0178
5	0.371	93	1.24	93	0.8793	0.0159
1	0.420	97	1.40	97	0.8183	0.0073

Table 1. Experimental data versus predictions of the percolation theory.